© Copyright, Princeton University Press. No part of this book may be distributed, posted, or reproduced in any form by digital or mechanical means without prior written permission of the publisher.

# 1 Introduction

Asteroseismology is the study of stellar pulsations. Stellar pulsations give us a unique window into the interiors of stars and provide us with the means to probe the internal structure, physical processes, and state of evolution of a star. This makes it possible to build a reliable, tested, and calibrated theory of stellar evolution. Asteroseismic data can give us precise estimates of the mass, radius, and ages of stars; in fact these data are the only means by which we can, in principle, obtain model-independent estimates of masses of single field stars.

In addition to the study of stellar physics, asteroseismic data have a range of applications in other fields of astrophysics. One of the most successful applications has been in the study of exoplanetary systems, where accurate properties of the host star are needed to fully characterize the newly discovered exoplanets. Another application is in the study of the structure and evolution of the Galaxy—Galactic archaeology—using the properties of red giants. Red giants are intrinsically bright and can be seen over large distances. Estimates of the radii of these stars can tell us about their luminosity and hence distance; estimates of their masses can be used to estimate their ages. Thus these stars can be used to determine the ages of stellar populations in different parts of the Galaxy.

## 1.1 THE DIFFERENT TYPES OF PULSATORS

Stellar pulsations may be detected by observing the variations of a star's brightness as a function of time. Radial velocity observations are also used in certain cases, though most pulsating stars have been studied using brightness variations. There is a long history of observing pulsating stars. One of the first known oscillating stars, *o* Ceti, was discovered in 1596. P Cygni was discovered soon thereafter in 1600. The first Cepheids, $\delta$ Cephei and $\eta$ Aquilæ, were discovered in 1784. And the other well-known pulsating star, RR Lyræ, was discovered in 1899. Since then, pulsating stars have been observed throughout the Hertzsprung-Russell (HR) diagram, and it appears that oscillations are a ubiquitous feature of stars.

The most well-known pulsating stars that have been observed over the years have two features in common: they have large amplitudes (and hence are easy to observe from the ground); and more importantly, most of the stars lie along a well-defined narrow strip on the $T_{\rm eff}$–luminosity plane, where $T_{\rm eff}$ is the effective temperature. The preponderance of pulsating stars in this region of the HR diagram

For general queries, contact webmaster@press.princeton.edu

© Copyright, Princeton University Press. No part of this book may be distributed, posted, or reproduced in any form by digital or mechanical means without prior written permission of the publisher.



has led it to be called the *instability strip*. These large-amplitude oscillators are usually self-excited (i.e., layers in the stars act as a heat engine). These layers can trap heat when the star is contracting and release it in the expansion phase, cooling the star and causing contraction again and thus allowing the cycle of pulsation to continue. For this mechanism to work, the pertinent layer has to be positioned at a suitable depth inside the star, which can happen for certain combinations of temperature and luminosity, with metallicity also playing a role. The most common cause of these oscillations is the position of the helium ionization zone—unlike other layers of stars, ionization zones become more opaque when heated. The position of iron ionization layers is important for pulsations in massive stars.

The focus of this book is, however, not the study of these well-known pulsators but stars with solar-like pulsations—the small-amplitude oscillations that are continually excited (in a stochastic manner) and damped by turbulence in the outer convection zones of the stars. Most stars with outer convection zones that have been investigated show evidence of these oscillations. Since they are not forced, the oscillations have very low amplitudes (e.g., a few parts per million in the case of stars like the Sun, up to a few parts per thousand for red giants). This is in stark contrast to some of the classical pulsators, as can be seen in Figure 1.1, where we show the light curves and oscillation spectra of a classical pulsator and a Sun-like star. Because of the weak oscillation amplitudes, asteroseismic studies of solar-type stars are a relatively new endeavor. Oscillations of this type were first detected on the Sun, and as a result stars showing them are usually termed *solar-like oscillators*. Some of the well-studied classes of oscillators are listed in Table 1.1.

Stellar oscillations are three dimensional in nature and thus to describe them, we need functions of radius, latitude, and longitude (i.e., $r$, $\theta$, and $\phi$). The angular dependence of the different modes of the small-amplitude, solar-like oscillations are usually described in terms of spherical harmonics, since these functions are a natural description of the normal modes of a sphere. The radial function is more complicated, as we shall see in Chapter 3. The oscillations are usually labeled by three numbers: the radial order $n$, the angular degree $l$, and the azimuthal order $m$. The quantities $l$ and $m$ characterize the spherical harmonic $Y_l^m$. Modes with $n = 0$ are the so-called fundamental or f modes, and are essentially surface gravity modes. The degree $l$ denotes the number of nodal planes that intersect the surface of a star, and $m$ is the number of nodes along the equator. The radial order $n$ can be any whole number and is the number of nodes in the radial direction. Positive values of $n$ are used to denote acoustic modes, that is, the so-called p modes (p for pressure, since the dominant restoring force for these modes is provided by the pressure gradient). Negative values of $n$ are used to denote modes for which buoyancy provides the main restoring force. These are usually referred to as g modes (g for gravity). Modes with $l = 0$ are the radial modes in which the stars expand or contract as a whole (often referred to as *breathing* modes), $l = 1$ are the dipole modes, $l = 2$ the quadrupole modes, $l = 3$ the octopole modes, and so on. For a spherically symmetric star, all modes with the same degree $l$ and order $n$ have the same frequency. Asphericities, such as rotation and magnetic fields, lift this degeneracy and give rise to frequency splitting of the modes, making the frequencies $m$ dependent. It should be noted that in the context of classical pulsators, the lowest-order radial (i.e., $l = 0$) mode is often referred to as the *fundamental* mode. These modes should not be confused with the f modes.

For general queries, contact webmaster@press.princeton.edu

© Copyright, Princeton University Press. No part of this book may be distributed, posted, or reproduced in any form by digital or mechanical means without prior written permission of the publisher.



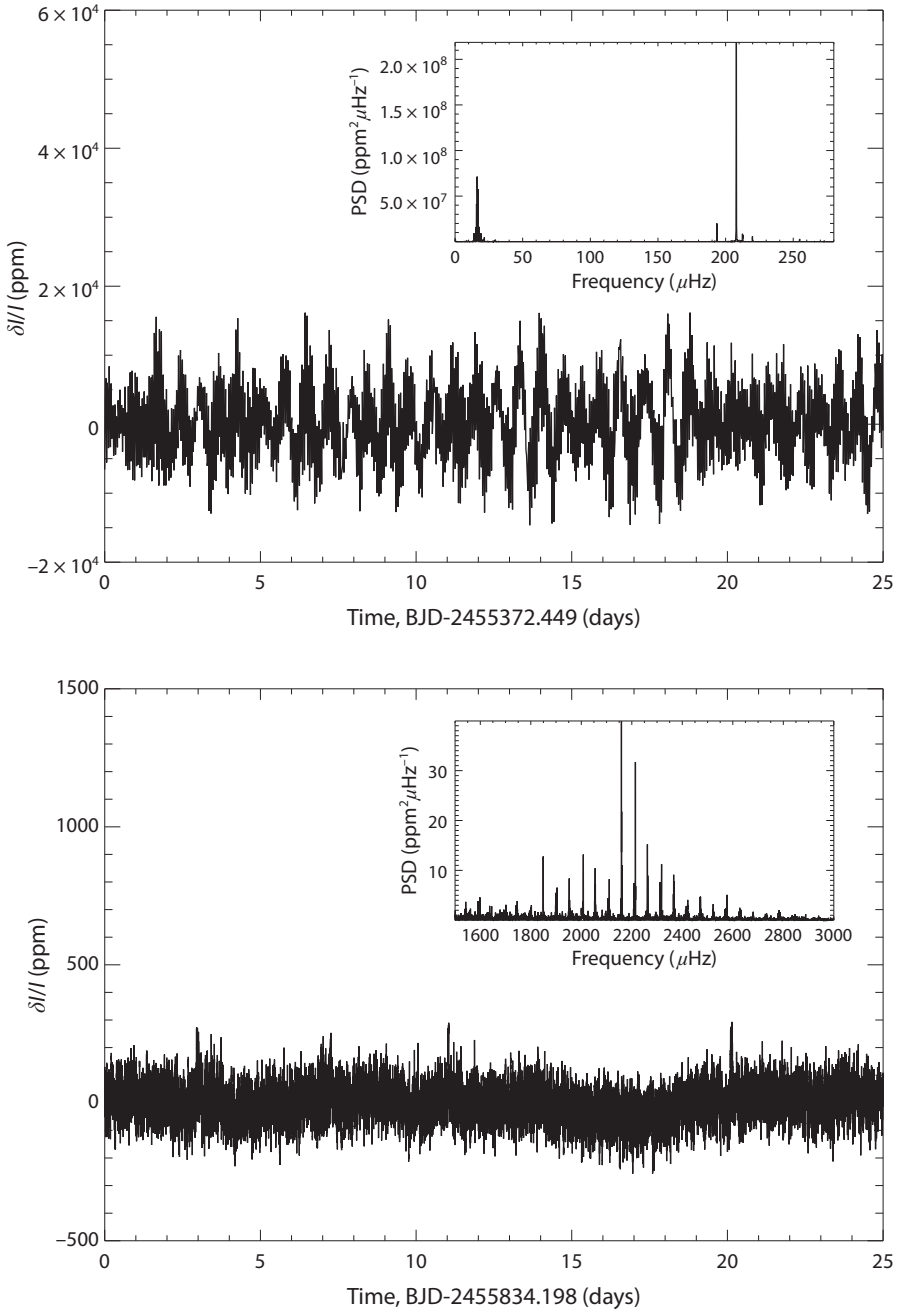


**Figure 1.1.** Top panel: A short segment of the *Kepler* lightcurve of a classical pulsator (KIC11145123) that shows both $\delta$ Scu and $\gamma$ Dor oscillations (see Table 1.1 for definitions) and a zoom of the oscillation spectrum. Bottom panel: A similar length segment, and oscillation spectrum, of the main sequence star 16 Cyg A (HD 186408). Note the much larger amplitudes and longer periods of the detected pulsations in the classical pulsator compared to the Sun-like star. Unlike the case of the classical pulsator, for 16 Cyg A the variance of the lightcurve is not dominated by the oscillations; the biggest contribution is from shot noise, with similar amplitude contributions arising from oscillations and surface convection (i.e., granulation).

For general queries, contact webmaster@press.princeton.edu

© Copyright, Princeton University Press. No part of this book may be distributed, posted, or reproduced in any form by digital or mechanical means without prior written permission of the publisher.



TABLE 1.1. TYPES OF PULSATORS

| Name | Properties |
|---|---|
| *On or near the main sequence* | |
| Solar-like pulsators | Main sequence stars like the Sun that are cool enough to have an outer convection zone; Low-amplitude, multiperiodic p-mode pulsators with periods of the order of minutes to tens of minutes |
| $\gamma$ Dor | Multiperiodic, periods of order 0.3–3 days; Lie at the intersection of the classical instability strip and the main sequence; Low-degree g-mode pulsators |
| $\delta$ Sct | Population I, multiperiodic, short periods of order 18 min to 8 hours; Lie at the intersection of the classical instability strip and the main sequence; Radial as well as nonradial p modes are observed |
| SX Phe | Same as $\delta$ Sct, but Population II stars |
| roAP | Rapidly rotating, highly magnetic, chemically peculiar A-type stars in the instability strip where $\delta$ Scuti stars are located; Multiperiodic, p-mode pulsations with periods of 5–20 min |
| SPB | Slowly pulsating B stars. Young Population I stars of about 8–18$M_{\odot}$; Similar to $\gamma$ Dor pulsators, with slower periods due to their larger size; g-mode pulsators with periods of 0.5–5 days |
| $\beta$ Cep | A short-period group of variables of spectral types B2–B3 IV–V; Can be multi-periodic; Periods of around 2–8 hours. Both p- and g-type pulsations are observed |
| Pulsating Be Stars | Oscillating Population I B-type stars that show Balmer-like emission; Generally have one dominant period but can be multi-periodic; Have high rotation rates and are often considered to be high rotation-velocity analogs of SPB and $\beta$ Cep stars |
| *Evolved stars* | |
| Solar-like pulsators | Stars in the subgiant, red giant or red-clump phases; Low-amplitude, multi-period oscillators with periods of minutes to hours; Stars oscillate in p modes and mixed modes (i.e., modes that are p-like at the surface and g-like in the core) |
| RR Lyræ | Low-mass Population II stars in the core-He burning stage; Radial mode pulsators with periods of about 0.3–0.5 days; Generally mono-periodic; Classified into three groups according to the skewness of the light-curve; Found in the classical instability strip |
| Cepheids | High-mass pulsators in the core-He burning phase; Generally mono-periodic radial-mode pulsations with periods of about 1–50 days, but can sometimes have have two periods; Found in the classical instability strip |
| W Virginis | Population II analogs of Cepheids; Found on the instability strip evolving toward the asymptotic giant branch; Divided into groups by period, with groupings of 1–5 days, 10–20 days, or longer than 20 days |
| RV Tauri | F to K supergiants; Can be called long-period W Virginis stars, but with some differences; Periods of 30–150 days; Lightcurves show alternating deep and shallow minima; Radial pulsations |

For general queries, contact webmaster@press.princeton.edu

© Copyright, Princeton University Press. No part of this book may be distributed, posted, or reproduced in any form by digital or mechanical means without prior written permission of the publisher.



TABLE 1.1. TYPES OF PULSATORS (*CONTINUED*)

| Name | Properties |
|---|---|
| Mira stars | Found near the tip of the giant branch, $1–7\times10^3 L_\odot$, with temperatures of 2,500 to 3,500 K. Generally long-period (hundreds of days to years) pulsations in the radial fundamental mode |
| Semiregular variables | Giants or supergiants of intermediate and late spectral types showing noticeable periodicity in their light changes accompanied by irregularities; Periods can be long, from 20 days to longer than 2,000 days; Usually subdivided into SRa, SRb, SRc, and SRd types according to periods and amplitudes; SRa stars are similar to Mira variables except that unlike the former, they oscillate in an overtone |
| *Compact stars* | |
| sdB stars | He burning stars that end up on the extreme horizontal branch because of mass loss; Masses less than $0.5M_\odot$, $T_{\rm eff}$ in the range $23–32\times10^3$ K, and $\log g$ between 5 and 6; There are two classes of these multiperiodic pulsators: p-mode pulsators with periods of 1–5 minutes, and g-mode pulsators with periods of 0.5–3 hours |
| *White dwarfs* | |
| GW Vir | DO type white dwarfs that pulsate; These stars have high $T_{\rm eff}$, in the range of $70–170\times10^3$ K; Multiperiodic, with periods of 7–30 min; Pulsate in g modes |
| DB stars | Cooler than GW Vir type stars, $T_{\rm eff}$ between 11 and $30\times10^3$ K; Periods of 4–12 min; Pulsate in g modes |
| DA stars | Also known as ZZ Ceti stars; Very narrow $T_{\rm eff}$ range around 11,800 K; Periods from less than 100 sec to longer than 1,000 sec; Pulsate in g modes |
| *Pre-main sequence stars* | |
| PreMS $\delta$ Scu | Pre-MS stars whose tracks cross the instability strip and show pulsations like $\delta$ Scu stars |
| PreMS $\gamma$ Dor | Pre-MS stars whose tracks cross the instability strip and show pulsations like $\gamma$ Dor stars |
| PreMS SPB | High-mass pre-MS stars that show SPB-like pulsations |

## 1.2 A BRIEF HISTORY OF THE STUDY OF SOLAR-TYPE OSCILLATIONS

The study of stochastically excited oscillators began with the Sun. Solar oscillations were first detected in the early 1960s. Later observations indicated that the detected oscillations were not merely surface phenomena. However, only in 1970 was a theoretical basis presented that interpreted the observations as standing waves trapped below the solar photosphere, a hypothesis fully confirmed by resolved observations of the Sun taken in the mid-1970s—observations that founded the field

For general queries, contact webmaster@press.princeton.edu

© Copyright, Princeton University Press. No part of this book may be distributed, posted, or reproduced in any form by digital or mechanical means without prior written permission of the publisher.



of helioseismology. Observational confirmation that the oscillations displayed by the Sun included truly global whole-Sun, core-penetrating pulsations followed in the late 1970s from observations made of the Sun as a star, (i.e., from observations in which the solar disc was not resolved).

The field of helioseismology developed rapidly beginning in the early 1980s. Dedicated ground-based networks were established to provide long, near-continuous observations of the Sun, allowing accurate and precise estimates of oscillation frequencies to be made and seismic studies of the solar activity cycle to be performed.

The first two dedicated networks made Sun-as-a-star observations. These observations do not resolve the solar disc, and hence their data are the most similar to the data we can get for other stars. The Birmingham Solar-Oscillations Network (BiSON) is still operating and continues to accumulate what is now a unique seismic record of the Sun stretching over more than three solar activity cycles. The International Research on the Interior of the Sun (IRIS) project collected similar data over several years. Next came the Global Oscillations Network Group (GONG), a network of six telescopes that make resolved-disc observations of the Sun, which therefore observes oscillations with short spatial scales on the solar surface. GONG started observing in 1995 and continues to operate.

Dedicated, long-term space-based observations followed soon after with the launch of the ESA/NASA Solar and Heliospheric Observatory (SoHO) in 1995. SoHO had three helioseismology-related instruments on board: the Michelson Doppler Imager (MDI), the Variability of solar Irradiance and Gravity Oscillations (VIRGO) package and the Global Oscillations at Low Frequencies (GOLF) spectrometer. Space-based observations are now being continued by the Heliospheric and Magnetic Imager (HMI) on board the Solar Dynamics Observatory (SDO).

Helioseismology has revolutionized our knowledge of the Sun. We know the structure and dynamics of the Sun in great detail thanks to these data. The data also show that the Sun changes with time; in particular, solar rotation in the outer layers changes with varying levels of solar activity. Describing what we have learned from helioseismology is beyond the scope of this book, but we have provided a reading list at the end of this chapter for those who may be interested in knowing more about this field.

The asteroseismic study of other solar-type stars took longer to develop because of the inherent difficulties of detecting extremely small variations of starlight from the ground, through the Earth's atmosphere. The first ground-based attempts were naturally focused on trying to detect pulsations in the very brightest main sequence and subgiant stars. In hindsight, the first detection of oscillations in a solar-type star was probably made in the early 1990s, when excess variability attributable to pulsations was observed in the subgiant Procyon ($\alpha$ CMi). At the time it was not possible to identify individual frequencies, and it would take observations made in the mid-1990s of another subgiant, $\beta$ Hyi, to finally reveal unambiguous evidence for individual oscillations in another solar-type star. Clear detections of oscillations in a Sun-like main sequence star, $\alpha$ Cen A, followed soon after.

Ground-based observations made at large telescopes present several logistical challenges, and only recently has a dedicated network for the study of solar-like oscillations been conceived—the Stellar Observations Network Group (SONG)—which is now being developed. However, it is the advent of dedicated, long-term observations by space-based missions that has truly revolutionized the observational

For general queries, contact webmaster@press.princeton.edu

© Copyright, Princeton University Press. No part of this book may be distributed, posted, or reproduced in any form by digital or mechanical means without prior written permission of the publisher.



field of asteroseismology by providing data of hitherto unseen quality on unprecedented numbers of stars. The story of space-based asteroseismology started with the ill-fated Wide-Field Infrared Explorer (WIRE). The satellite failed, because coolants meant to keep the detector cool evaporated. However, it was soon realized that the star tracker could be used to monitor stellar variability and hence to look for stellar oscillations. This led to observations of $\alpha$ UMa and $\alpha$ Cen A. The Canadian mission Microvariability and Oscillations of Stars (MOST) was the first successfully launched mission dedicated to asteroseismic studies. Although it was not very successful in studying solar-type stars, it was immensely successful in studying giants, classical pulsators, and even starspots and exoplanets.

The major breakthroughs for studies of solar-like oscillators came with the CNRS/ESA CoRoT Mission and the NASA *Kepler* Mission. CoRoT observed many cool red giants and showed that these stars show nonradial pulsations; the mission observed some cool subgiants and main sequence stars for asteroseismology. *Kepler* increased significantly the numbers of subgiants and main sequence stars with detected oscillations, increased the sample for red giants, and also heralded an epoch of ultraprecise analyses made possible by observations lasting up to the 4-year duration of the nominal mission. Studies of pulsations in these types of stars are continuing with the repurposed *Kepler* mission, K2, which is providing data on targets in many different fields near the ecliptic plane.

Asteroseismology is going through a phase of rapid development in which we are still learning the best ways to analyze and interpret the data. With two more space missions being planned that will provide more exquisite asteroseismology data—the NASA Transiting Exoplanet Survey Satellite (TESS; launch 2018), and the ESA Planetary Transits and Oscillations of stars (PLATO; launch 2025) missions —this field is going to grow even more rapidly.

## 1.3 OVERVIEW OF THE DATA

While various aspects will be explored in detail in subsequent chapters, our aim in what remains of this chapter is to give a brief introduction to the basic appearance and properties of the pulsation spectra of solar-like oscillators.

As noted above, stars with near-surface convection zones show solar-like oscillations, modes that are stochastically excited and intrinsically damped by the near-surface convection. While this process limits the amplitudes of these intrinsically stable modes, many overtones are often excited to detectable levels. The modes in cool main sequence stars are predominantly acoustic in nature (i.e., they are p modes). The top panel of Figure 1.2 shows the frequency-power spectrum of the *Kepler* lightcurve of the G-type main-sequence star 16 Cyg A (HD 186408), the more massive component of the Sun-like binary system 16 Cygni. When oscillations are clearly detected, as is the case here, we see a rich pattern of peaks at the frequencies of the high-overtone (order $n$), low-degree (low-$l$) p modes of the star. Both radial and nonradial modes are present (bottom-left panel). However, because of geometric cancellation, only modes of low degree can be observed, and even then some of the rotationally split $m$ components may be unobservable, depending on the angle of inclination of the rotation axis of the star. If we extend the plotted range of the spectrum to lower frequencies (bottom-right panel), we also see evidence of

For general queries, contact webmaster@press.princeton.edu

© Copyright, Princeton University Press. No part of this book may be distributed, posted, or reproduced in any form by digital or mechanical means without prior written permission of the publisher.



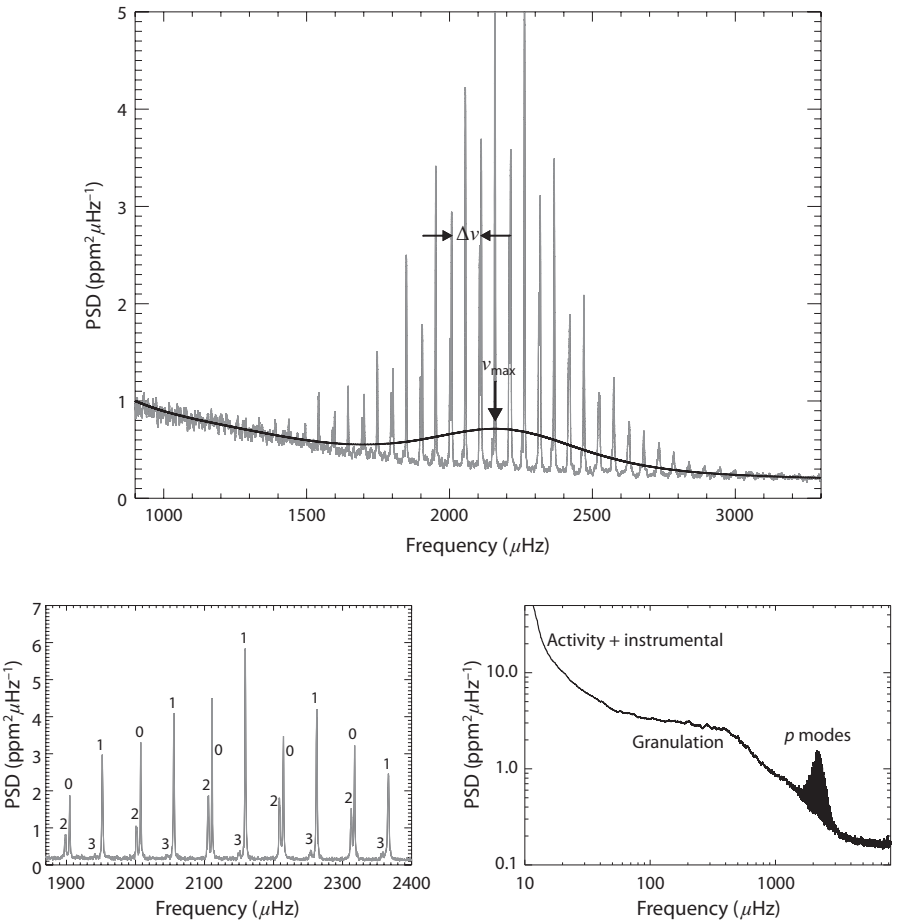


**Figure 1.2.** Frequency-power spectrum of the *Kepler* lightcurve of 16 Cyg A (HD 186408). Top panel: Lightly smoothed spectrum in gray, heavily smoothed in black, showing the Gaussian-like power envelope. Bottom-left panel: Zoom of the central part of the spectrum, with annotation showing the angular degree $l$ of each mode. Bottom-right panel: Logarithmic plot of a wider frequency range, showing contributions from granulation, activity, and instrumental noise.

signatures of the surface patterns of convection (granulation) and the evolution of starspots (magnetic activity), in addition to contributions due to instrumental noise (e.g., drifts).

The power due to the oscillations is modulated in frequency by an envelope that typically has a Gaussian-like shape. The oscillation spectrum of 16 Cyg A is a classic example (top panel, Figure 1.2). We note in passing that there is growing evidence suggesting that oscillation power envelopes in the hottest (F-type) and coolest (K-type) solar-like oscillators tend to be flatter in shape. The frequency at which the observed power is strongest is called $\nu_{max}$. This global asteroseismic parameter is a useful diagnostic of the physical properties of the near-surface layers of the star. As we will see in Chapter 3, it is related to the acoustic cutoff frequency of a star which,

For general queries, contact webmaster@press.princeton.edu

© Copyright, Princeton University Press. No part of this book may be distributed, posted, or reproduced in any form by digital or mechanical means without prior written permission of the publisher.



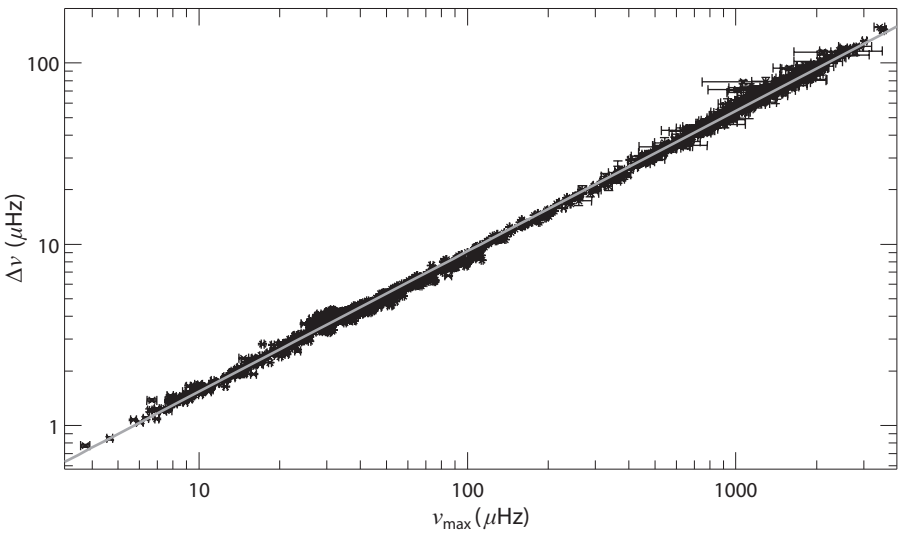


**Figure 1.3.** The observed relation between $\Delta\nu$ and $\nu_{\max}$ of some stars observed by the *Kepler* mission. The gray line is a least-squares fit to the data. The fit implies that $\Delta\nu \propto \nu_{\max}^{0.77}$.

with a few assumptions, implies a dependence on intrinsic properties of the form $\nu_{\max} \propto g\, T_{\rm eff}^{-1/2}$.

Another important global seismic parameter is the average large-frequency separation, $\Delta\nu$ (top panel, Figure 1.2). It is an average of the frequency differences

$$\Delta\nu_{nl} = \nu_{n+1,l} - \nu_{n,l} \tag{1.1}$$

between consecutive overtones $n$ of the same degree $l$. The observed average separation scales to very good approximation as $\bar{\rho}^{1/2}$, with $\bar{\rho} \propto M/R^3$ being the mean density of a star of mass $M$ and surface radius $R$. This dependence follows if we assume that (1) the observed average separation is close to the separation in the asymptotic relation for p modes discussed in Chapter 3 and (2) we may treat stars as homologously scaled versions of one another. The average large separation and the frequency of maximum power are related, as can be seen in Figure 1.3. This is not completely surprising since both $\Delta\nu$ and $\nu_{\max}$ depend on the global properties of a star. We shall examine the theoretically expected relation between the two parameters in Chapter 3.

The near-regular nature of the patterns of frequencies shown by main sequence stars may also be shown in the form of an échelle (ladder) diagram, like the one in Figure 1.4. It was made by dividing the spectrum of 16 Cyg A into frequency segments of length $\Delta\nu$. The segments were then stacked in ascending order, and the frequencies of the low-$l$ modes were marked in each segment on the resulting diagram (see the different plotting symbols in the figure). Formally, we have plotted $\nu_{nl}$ against the wrapped (reduced) frequencies ($\nu_{nl}$ mod $\Delta\nu$). Note that when the diagram is constructed in this way, modes in a given order $n$ lie on lines that slope upward, as shown by the dotted lines. The orders can be made horizontal if the frequencies plotted on the vertical axis are instead those at the center of each order.

For general queries, contact webmaster@press.princeton.edu

© Copyright, Princeton University Press. No part of this book may be distributed, posted, or reproduced in any form by digital or mechanical means without prior written permission of the publisher.



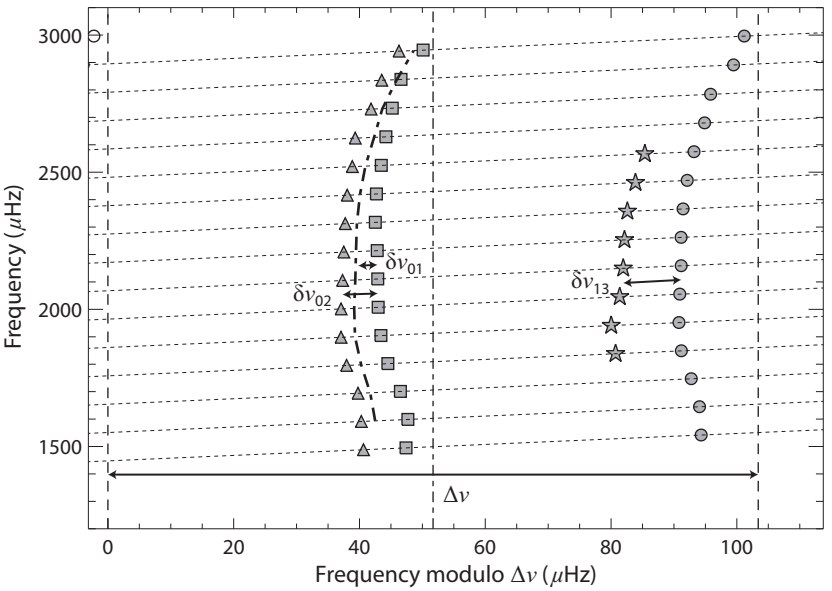


**Figure 1.4.** Échelle diagram of the oscillation frequencies of 16 Cyg A, with $l = 0$ modes plotted as squares, $l = 1$ modes as circles, $l = 2$ modes as triangles, and $l = 3$ modes as stars. Dotted lines follow the sloping orders. The heavy dot-dashed line follows the exact halfway frequencies between adjacent $l = 1$ modes. The vertical dashed lines mark zero and $\Delta\nu$ on the abscissa, and the thin dot-dashed line marks $\Delta\nu/2$. Characteristic frequency separations are also marked on the plot (see text).

The diagram shows clear *ridges*, each one comprising overtones of a different degree. Departures from strict regularity of the frequency spacings are revealed by curvature in the ridges. As we shall see later, this carries important information on the underlying structure of the star. In addition to $\Delta\nu$, we have also marked three characteristic small frequency separations on the diagram. Shown are the separations between adjacent $l = 0$ and 2 modes $[\delta\nu_{02}(n)]$, and between adjacent $l = 1$ and $l = 3$ modes $[\delta\nu_{13}(n)]$; $\delta\nu_{01}(n)$ measures deviations of the $l = 0$ modes from the exact halfway frequencies of the adjacent $l = 1$ modes ($\delta\nu_{10}(n)$ gives the separations with the mode degrees swapped). These small-frequency separations depend on the gradient of the sound speed in the deep interior of the star, and in main sequence stars provide a sensitive diagnostic of age (for a given assumed physics and chemical composition).

As main sequence stars evolve, the observed oscillations move to lower frequencies (i.e., $\nu_{\max}$ decreases), largely in response to the decreasing surface gravity. Figure 1.5 shows frequency spectra of five solar-like oscillators observed by *Kepler* (including 16 Cyg A, the second star down), which all have similar masses to that of the Sun. The stars are arranged from top to bottom in order of decreasing $\nu_{\max}$ (i.e., increasing evolutionary state). The top two stars are on the main sequence. The third and fourth stars are subgiants and therefore have finished burning hydrogen in their cores; the fifth star lies at the base of the red-giant branch.

Once stars leave the main sequence and enter the subgiant phase, they begin to show detectable signatures of gravity (g) modes, where the effects of buoyancy

For general queries, contact webmaster@press.princeton.edu

© Copyright, Princeton University Press. No part of this book may be distributed, posted, or reproduced in any form by digital or mechanical means without prior written permission of the publisher.



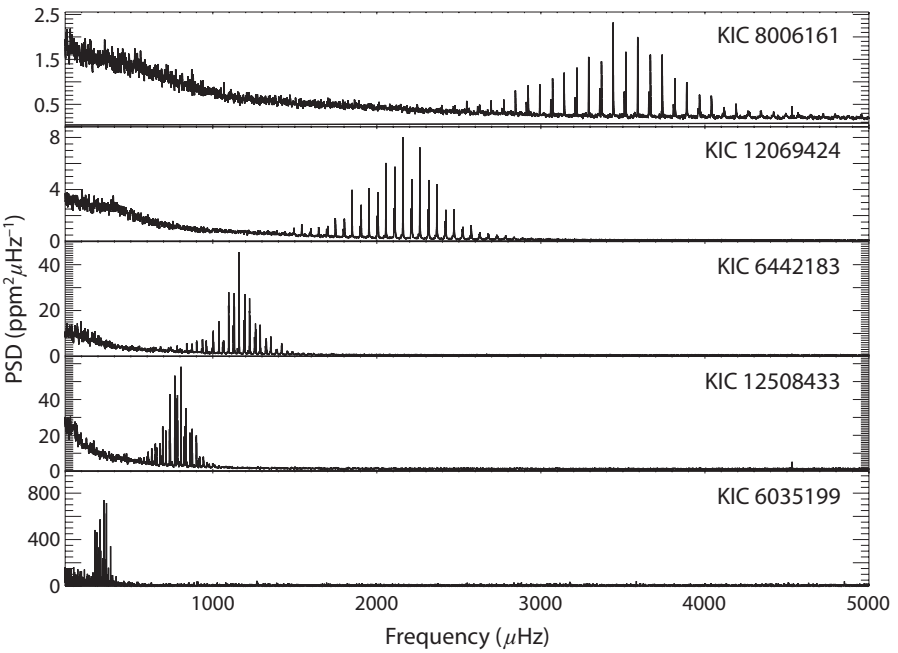


**Figure 1.5.** Frequency-power spectra of five solar-like oscillators observed by *Kepler*, which all have similar masses to that of the Sun. The stars are arranged from top to bottom in order of decreasing $\nu_{\max}$.

provide the restoring force. In a stable (nonconvective) layer, a small displacement of a parcel of fluid will cause it to oscillate with a frequency known as the Brunt-Väisälä frequency (or buoyancy frequency). As we shall see later, the Brunt-Väisälä frequency is the highest frequency that a g mode can have, and in the deep stellar interior it increases during the post–main sequence phase, eventually extending into the frequency range of the detectable, high-order p modes. When the frequency of a g mode comes close to that of a nonradial p mode of the same degree $l$, the modes interact, or couple, and undergo an avoided crossing (analogous to avoided crossings of atomic energy states). Interactions between the modes not only "bump" (shift) the observed frequencies but also change the intrinsic character of the modes so that they take on mixed p- and g-mode characteristics, having g-mode-like behavior in the deep interior and p-mode behavior in the envelope.

Figure 1.6 shows the échelle diagram of the oscillation frequencies of HD 183159 (KIC 6442183), the third star down in Figure 1.5. Note how we have copied, or replicated, the échelle into the ranges $\{-\Delta\nu, 0\}$ and $\{\Delta\nu, 2\Delta\nu\}$, where the frequencies are plotted with open symbols. For this star we have a single pure g-mode—which has a frequency of about 1,000 $\mu$Hz—that has moved into the detectable p-mode range, and hence we see the effects of several $l = 1$ p modes coupling to it. The interactions manifest in the frequency pattern as an avoided crossing, with some of the $l = 1$ overtones being shifted significantly from the putative undisturbed $l = 1$ ridge. This includes two modes that have been shifted all the way across to the $l = 0$ ridge. There is one extra $l = 1$ mode at each avoided

For general queries, contact webmaster@press.princeton.edu

© Copyright, Princeton University Press. No part of this book may be distributed, posted, or reproduced in any form by digital or mechanical means without prior written permission of the publisher.



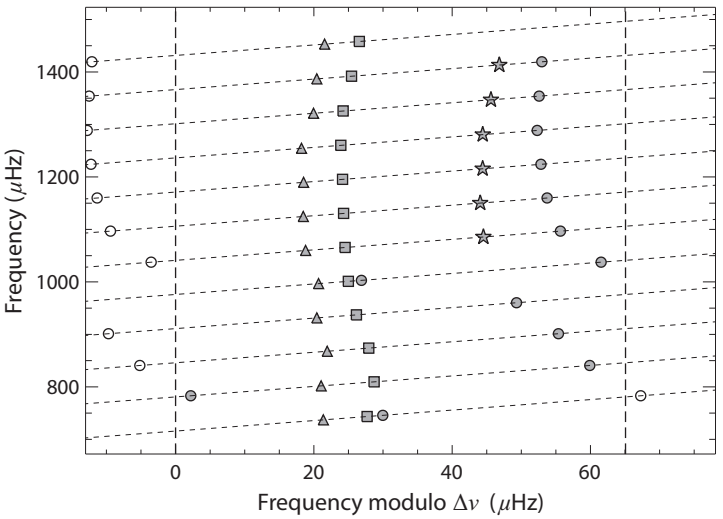


**Figure 1.6.** Échelle diagram of the oscillation frequencies of HD 183159 (KIC 6442183; third star down in Figure 1.5), with $l = 0$ modes plotted as squares, $l = 1$ modes as circles, $l = 2$ modes as triangles, and $l = 3$ modes as stars. Modes are plotted with open symbols where the échelle repeats.

crossing, implying a reduction in the frequency spacings between the relevant dipole modes. The frequency of the avoided crossing corresponds to the pure g-mode frequency that the star would show if it were comprised only of the central g-mode cavity; this freguency is a sensitive diagnostic of the core properties and the exact evolutionary state (again, for a given assumed physics and chemical composition).

Whereas in the above example we had a single g mode coupling to several p modes, as stars evolve into the red-giant phase, the increased density (in frequency) of g modes in the high-order p-mode regime leads to a much richer set of interactions and observable signatures. As we will see later, these signatures may be used to discriminate different advanced phases of evolution. As a foretaste, Figure 1.7 shows the frequency spectrum and échelle diagram of a star on the red-giant branch. *Kepler*-432 is a low-luminosity red giant that hosts a transiting Jupiter-sized planet, as well as a nontransiting gas giant revealed by ground-based Doppler velocity observations, which lies in a wider orbit. The annotation in the left panel of Figure 1.7 shows where the modes of different degrees of the star lie in its oscillation spectrum. In each order, we have several closely spaced g modes coupling to a single p mode, which gives rise to clusters of mixed $l = 1$ modes occupying the gray regions. The échelle diagram shows clearly that there are now several mixed modes in each order.

The quantities $\Delta\nu$, $\nu_{\rm max}$, and the individual frequencies form the basis of all asteroseismic analyses. While the two parameters $\Delta\nu$ and $\nu_{\rm max}$ are usually enough to determine the mass and radius of the star, the individual frequencies provide more refined estimates and are also needed for modeling the interior. In this book we describe how we use these data to determine properties of a star.

For general queries, contact webmaster@press.princeton.edu

© Copyright, Princeton University Press. No part of this book may be distributed, posted, or reproduced in any form by digital or mechanical means without prior written permission of the publisher.



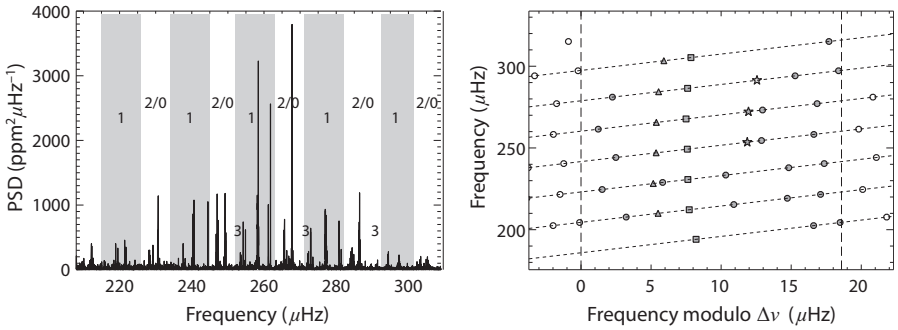


**Figure 1.7.** Left panel: Frequency-power spectrum of the planet-hosting star *Kepler*-432. The annotation marks where modes of different degree lie, including clusters of mixed $l = 1$ modes (gray regions). Right panel: Échelle diagram of the frequencies of *Kepler*-432, with $l = 0$ modes plotted as squares, $l = 1$ modes as circles, $l = 2$ modes as triangles and $l = 3$ modes as stars.

## 1.4 SCOPE OF THIS BOOK

The analysis of asteroseismic data obtained by *Kepler* has resulted in the development of specialized techniques to analyze and interpret the data. This book is a distillation of some of the techniques that are used. It is aimed at students and researchers who want to enter the field and at other astrophysicists who simply want to know how asteroseismic analyses are carried out. Instructors of senior undergraduate and graduate classes will also find this book useful. Although we do discuss the equations governing stellar structure and evolution, we expect that readers already have some knowledge of stellar theory and hence are familiar with the different stages of evolution of a star.

We start the main part of the book with a brief discussion of the equations of stellar structure in Chapter 2 and then derive the equations that govern stellar pulsations in Chapter 3. We also discuss some properties of the oscillations. Since there are texts that deal solely with the equations of stellar pulsations and their properties, we have limited ourselves to what we consider to be the bare minimum that a student needs to know to embark on this field. Chapters 2 and 3 on theory are followed by Chapters 4–9 on data analysis and interpretation. In Chapters 4–6 we discuss the basic content of observed time series of stellar brightness (or velocity) data on stars, why these data look like they do, and how they are analyzed to extract the asteroseismic parameters. In Chapters 7–9 we explain the different ways in which stellar properties are determined. These chapters are followed by Chapter 10 on inversions. Inversions have been successfully used by helioseismologists to construct a detailed picture of the internal structure and dynamics of the Sun and also some aspects of variations of its structure over time. Inversions of frequencies and frequency splittings of other stars are still in their infancy. However, because inversions give model-independent estimates of stellar structure, we include a fairly detailed description of inversion techniques.

Perhaps the most rapidly evolving part of this field is red-giant asteroseismology. Until comparatively recently it was assumed that red giants would not show nonradial oscillations. What CoRoT and then *Kepler* have shown is not only that nonradial oscillations are present, but also that they are detectable in such numbers

For general queries, contact webmaster@press.princeton.edu

© Copyright, Princeton University Press. No part of this book may be distributed, posted, or reproduced in any form by digital or mechanical means without prior written permission of the publisher.



that make the oscillation spectra notably richer and more complicated than those shown by main sequence stars. While we have not treated red giants in a separate chapter, wherever necessary we have discussed how red giants require different analysis techniques. Because of the rapid evolution of the field, the discussion on red giants will inevitably be incomplete.

## 1.5 FURTHER READING

This book deals exclusively with stochastically excited pulsators. The ways in which data from heat-engine pulsators are analyzed is often very different from the analysis techniques presented in this book. Readers interested in learning more about heat-engine pulsators are referred to the following books:

- Christensen-Dalsgaard, J., 2003, *Lecture Notes on Stellar Oscillations*, Aarhus University. Available online at http://astro.phys.au.dk/∼jcd/oscilnotes/.
- Balona, L. A., 2010, *Challenges in Stellar Pulsation*, Bentham Publishers.
- Aerts, C., Christensen-Dalsgaard, J., and Kurtz, D. W., 2011, *Asteroseismology*, Springer.
- Catelan, M., and Smith, H. A., 2015, *Pulsating Stars*, Wiley-VCH.

For first-hand accounts of the development of helioseismology, readers can look at articles in:

- Jain, K., Tripathy, S. C., Hill, F., Leibacher, J. W., and Pevtsov, A. A., eds., 2013, *Fifty Years of Seismology of the Sun and Stars*, *ASP Conference Series*, **478**.

A nontechnical introduction to helioseismology can be found in:

- Chaplin, W. J., 2006, *Music of the Sun: The Story of Helioseismology*, Oneworld Publications.

Most available helioseismic data have been extracted from disc-resolved observations of the Sun, and as a result, the techniques used to extract helioseismic frequencies are very different from what we shall discuss in the following chapters. Readers interested in how such data are analyzed are referred to the following articles:

- Anderson, E. R. Duvall, T. L., and Jeffries, S. M., 1990, *Modeling of Solar Oscillation Power Spectra*, *Solar Physics*, **364**, 699.
- Hill, F. et al., 1996, *The Solar Acoustic Spectrum and Eigenmode Parameters*, *Science*, **272**, 1292.
- Larson, T., and Schou, J., 2011, *HMI Global Helioseismology Data Analysis Pipeline*, *J. Phys. Conference Series*, **271**, 012062.
- Reiter, J. et al., 2015, *A Method for the Estimation of p-Mode Parameters from Averaged Solar Oscillation Power Spectra*, *Astrophys. J.*, **803**, 92.
- Korzennik, S. G., et al., 2013, *Accurate Characterization of High-Degree Modes Using MDI Observations*, *Astrophys. J.*, **772**, 87.

Helioseismology has revealed details of solar structure and dynamics. Helioseismic analyses have also allowed us to use the Sun as a laboratory. The following reviews describe what helioseismology has taught us about the Sun:

- Christensen-Dalsgaard, J., 2002, *Helioseismology*, *Rev. Mod. Phys.*, **74**, 1073.
- Gizon, L., and Birch, A. C., 2005, *Local Helioseismology*, *Living Rev. Solar Phys.*, **2**, 6.

For general queries, contact webmaster@press.princeton.edu

© Copyright, Princeton University Press. No part of this book may be distributed, posted, or reproduced in any form by digital or mechanical means without prior written permission of the publisher.



- Chaplin, W. J. and Basu, S., 2008, *Perspectives in Global Helioseismology and the Road Ahead*, *Solar Phys.*, **251**, 53.
- Howe, R., 2009, *Solar Interior Rotation and Its Variation*, *Living Rev. Solar Phys.*, **6**, 1.
- Basu, S., 2016, *Global Seismology of the Sun*, *Living Rev. Solar Phys.*, **13**, 2.

To learn a little about the development of asteroseismology, the following articles are useful:

- Brown, T. M., and Gilliland, R. L., 1994, *Asteroseismology*, *Ann. Rev. Astron. Astrophys.*, **32**, 37.
- Christensen-Dalsgaard, J., 2004, *An Overview of Helio- and Asteroseismology*, *Helio- and Asteroseismology: Towards a Golden Future*, Proc. *SoHO* 14/GONG 2004 Workshop, ESA SP 559, European Space Agency.
- Chaplin, W. J., and Miglio, A., 2013, *Asteroseismology of Solar-Type and Red-Giant Stars*, *Ann. Rev. Astron. Astrophys.*, **51**, 353.

## 1.6 EXERCISES

**1**. Find the mean density of stars with $\Delta\nu$ values listed below. Assume that $\Delta\nu_\odot = 135\,\mu$Hz:

(a) 123.41 $\mu$Hz
(b) 120.04 $\mu$Hz
(c) 80.81 $\mu$Hz
(d) 55.72 $\mu$Hz
(e) 29.44 $\mu$Hz
(f) 12.09 $\mu$Hz
(g) 9.630 $\mu$Hz

Can you identify the dwarfs and giants in the sample?
**2.** Given the $\Delta\nu$ and $\nu_{\rm max}$ scaling relations, derive expressions for mass and radius. Derive the uncertainty in the estimated mass and radius in terms of uncertainties in $\Delta\nu$, $\nu_{\rm max}$, and $T_{\rm eff}$.
**3.** Frequencies of evolutionary sequences of stellar models of masses $1.40M_\odot$ and $1.5M_\odot$ are given in archive `frequencies_ov2.tar.gz`[1]. The properties of the models may be found in file `properties_ov2.txt`. Draw the échelle diagram for each model, and explore how evolution changes the diagram.
**4.** Mode-frequencies of several stars observed by *Kepler* may be found in the archive `obs_freq.tar`. Draw the échelle diagram for each star and using the diagrams, infer which evolutionary stages the stars are in.

[1]Links to this and other online materials adjust to this book can be found at http://press.princeton.edu/titles/11170.html.

For general queries, contact webmaster@press.princeton.edu